

# Future Land-use Changes in the transboundary Sio-Malaba-Malakisi Basin of East Africa: Simulations using the CLUE-S model and Classified Satellite Land Cover Datasets

Stanley Chasia<sup>a</sup>, Luke Olang<sup>b,c</sup>, Lewis Sitoki<sup>a</sup>

<sup>a</sup>Department of Geosciences and Environment, Technical University of Kenya, Nairobi, Kenya,  
P.O. Box 52428 – 00200 Nairobi, Kenya

<sup>b</sup>Department of Biosystems and Environmental Engineering, Technical University of Kenya,  
Nairobi, Kenya, P.O. Box 52428 – 00200 Nairobi, Kenya

<sup>c</sup>Centre for Integrated Water Resource Management, Technical University of Kenya, Nairobi,  
Kenya, P.O. Box 52428 – 00200 Nairobi, Kenya

Corresponding Author Email: stanley.chasia@tukenya.ac.ke  
P.O. Box 52428 – 00200 Nairobi, Kenya

## Abstract

A comprehensive understanding of land-use/cover(LUC) change processes, their trends and future trajectories is essential for the development of sustainable land-use management plans. While contemporary tools can today be employed to monitor historical land-cover changes, prediction of future change trajectories in most rural agro-ecological landscapes remains a challenge. This study evaluated potential LUC changes in the transboundary Sio-Malaba-Malakisi River Basin of Kenya and Uganda for the period 2017-2047. The land use change drivers were obtained through a rigorous fieldwork procedure and the Logistic Regression Model (LGM) to establish key factors for the simulation. The CLUE-S model was subsequently adapted to explore future LUC change trajectories under different scenarios. The model was validated using historical land cover maps for the period of 2008 and 2017, producing overall accuracy result of 85.7% and a Kappa coefficient of 0.78. The spatial distribution of vegetation cover types could be explained partially by proximate factors like soil cation exchange capacity, soil organic carbon and soil pH. On the other hand, built-up areas were mainly influenced by population density. Under the afforestation scenario, areas under forest cover expanded further occupying 54.7% of the basin. Conversely, under the intense agriculture scenario, cropland and pasture cover types occupied 78% of the basin. However, in a scenario where natural forest and wetlands were protected, cropland and pasture only expanded by 74%. The study successfully outlined proximate land cover change

drivers, including potential future changes and could be used to support the development of sustainable long-term transboundary land-use plans and policy.

**Key words:** Land-use Change - CLUE-S Model - Scenario analysis - Transboundary Basin - East Africa

## **1 Introduction**

Land use changes are universal earth processes of global importance and environmental change research (Cegielska et al., 2018; Chen et al., 2019; Duveiller et al., 2020; Thenkabail, 2016). They manifest locally but cumulatively affect the sustainability and proper functioning of Earth's land surface processes (Midekisa et al., 2017; Song et al., 2018) and system functioning (Lambin et al., 2001). The net effects of Land Use Land Cover Changes (LULCC) on socio-economic activities and the well-being of environments are manifested differently in different geographical settings. However, the outcome is generally similar exhibiting both short-term and long-term impacts (Foley et al., 2005; Marcos-Martinez et al., 2017). Generally, the effects of land-use change may lead to loss of critical biodiversity (Newbold et al., 2015), land degradation (Olang et al., 2014), global climate change (Duveiller et al., 2020) and habitat destruction (Ban et al., 2015; Du & Huang, 2017). At local scales, these may lead to loss of soil productivity, alterations of local hydrological regimes (Olang et al., 2014), increasing risk of hazards like landslides (Lambin et al., 2001), soil erosion and water pollution (Duveiller et al., 2020; Newbold et al., 2015; Schürz et al., 2020). Socio-economic impacts of land use change may also arise from loss of livelihoods, increased vulnerability to food insecurity and land related conflicts (Lone & Mayer, 2019).

In sub-Saharan Africa where rain-fed agriculture is the dominant socio-economic activity (Maitima et al., 2009), the negative feedback from land-use changes and impacts on people's livelihoods are usually more pronounced and immediately felt by small-holder farmers and local communities (Hartemink & van Keulen, 2005; Karamage et al., 2017; Lambin & Ehrlich, 1997). The overall increase in human population exerts more pressure on the limited productive land resource leading to intensification of farming activities on small parcels of land and accelerating the rate of degradation (Fetzel et al., 2016; Vanwalleghem et al., 2017). In some cases, farming activities have shifted or expanded to ecologically fragile areas and other protected habitats thus threatening ecosystem functions and stability thus completing the "cycle" of destruction (Karamage et al., 2017). In smaller catchment areas, the negative effects of LUCC changes take the form of upstream-downstream conflicts (Fayos, 2002). On the other hand, in transboundary catchments setting like the SMM basin, this becomes a serious issue of

international concern involving different political jurisdictions with the potential to instigate bilateral conflicts between neighboring states(Petursson et al., 2011).

Land use-change studies attempt to qualitatively and quantitatively measure LULC changes at different spatiotemporal scales using available satellite data (Ban et al., 2015) and field measurement techniques(Congalton et al., 2014). Understanding the impacts of LUCC involves unpacking and assessing the complex interrelationships between the biophysical and socio-economic factors involved using empirical models and scientific tools (Behera & Behera, 2020). However, developing sustainable land-use management plans and policy in the long-term requires an assessment of future land-use trajectories using techniques that extrapolate trends and perform scenario analysis (Briassoulis, 2019). Land-use change models provide a means to explore and simplify the complex spatiotemporal relationships between LUCC and potential driving factors (Briassoulis, 2019; Peter H Verburg et al., 2004). Empirical and spatially explicit models have been developed to study spatial patterns of LULC and therefore acting as decision support tools, an explanatory means of observed relationships, prediction and impact assessment tools (Briassoulis, 2019; UNDP, 2018; Peter H. Verburg et al., 2002, 2019).

Several models have been developed across the globe for assessing LULC changes and understanding the complex linkages and feedbacks between these changes and potential driving factors (Chaudhuri & Clarke, 2013; Irwin & Geoghegan, 2001; Matthews et al., 2007; van Soesbergen & MacArthur Foundation, 2016). Yirsaw et al., (2017) for instance used the CA-Markov(Cecullar Automata) model to explore future LULC changes in China and predict ecosystem services values (ESV) for each LULC category. The model was able to predict how each ESV was affected by different LULC activities over the course of the study period. However, (Liping et al., 2018) used the same model in a similar geographical setting but prediction results were affected by limited data availability. Saxena & Jat, (2019) applied the SLEUTH model, which is a CA-based model to capture the heterogenous urban landscape in India and recorded satisfactory results that highlighted different forms of urban development. However, the model could not capture small unit fragments of growth. Schulp et al., (2019) on the other hand used an integrated approach by combining macro-economic, sectoral and land use allocation model (Dyna-CLUE) to simulated land use changes in the cultural landscapes in Europe. Their study was able to establish the co-occurrence of land trajectories and cultural landscape types. However, local change processes affecting cultural landscape were not well represented.

The Conversion of Land use/cover and its Effects at Small regional extent (CLUE-S) model (Peter H. Verburg & Overmars, 2009) has also been used as a tool to model future changes in LULC given a set of explanatory factors that drive the changes (P.H. Verburg & Overmars, 2007; Peter H. Verburg et al., 2002). CLUE-S model has been used in hydrological studies (Peng et al., 2020; Waiyasusri et al., 2016; Wang et al., 2021; Zhou et al., 2013), land cover change dynamics and environmental studies (Behera & Behera, 2020; Griscom et al., 2010; Kucsicsa et al., 2019; Mohammady et al., 2018; P.H. Verburg & Overmars, 2007) and urban studies (Huang et al., 2019; Jiang et al., 2015). In southern Spain, (Claessens et al., 2009) coupled the CLUE model with a landscape process model to investigate the interactions between LULC and landscape dynamics. In Africa, the CLUE-S model has been applied in various studies. For instance, (Judex & Menz, 2006), used different scenarios to model land-cover changes in a West African catchment using the CLUE-S framework. The model was able to produce realistic model predictions of the study using available biophysical and field data. In a similar study, (Tizora et al., 2018) applied the Dyna-CLUE model to simulate LULC change in South Africa and achieved results that indicated a good simulation fit between model results and reference map.

The CLUE-S model was therefore adopted in this study to model land use-cover changes in SMM basin by first identifying important biophysical and socio-economic driving factors based on trend extrapolation using historical land-cover change data for the past thirty years to model future change trajectories under different realistic scenario conditions. The findings will contribute scientific knowledge and information to the ongoing land management efforts in the basin and provide critical baseline data to support a transboundary and integrated land-use planning framework that fosters sustainable development

## **2 Materials and Methods**

### **2.1 The Study Area**

The study was carried out in Sio-Malaba-Malakisi catchment located on the border region between Kenya and Uganda (Fig. 1). It covers approximately 2,605 km<sup>2</sup>, and extends from 1°5'10" N, 34°6'10" E and 0°14'45" N, 34°36'25" E. The upper reaches of the catchment, form the headwaters of rivers Malakisi, Malaba and Sio, flowing southwards towards Lake Victoria. The altitude range between approximately 1100 to 4,200 m. The study area experiences a bimodal rainfall pattern (Alemayehu et al., 2017), with a mean annual rainfall of approximately 1500 – 2000mm (Reed & Clokie, 2000; Wanyama et al., 2020), characterized by a period of “long-rains”

(March – May), and “short-rains” (October – December) (Ongoma et al., 2018). This coincides with the passage of north-south/south-north intertropical convergence zone (ITCZ) (Camberlin & Okoola, 2003; Yang et al., 2015). Vegetation distribution is influenced by altitude, and is comprised of montane forest, bushland and grassland communities (Reed & Clokie, 2000). The rich volcanic soils support crop cultivation, mainly maize, soy beans, sorghum, millet, rice, peanuts, and vegetables. Coffee, sugarcane and cotton are important cash crops in the area. The largely agrarian population, is approximated to be 192 persons km<sup>-2</sup>, by data from both Uganda Bureau and Kenya Bureau of statistics. This population occupies a potential arable land of less than 60% of the total basin area, thus exerting pressure on the limited land resource.

The Sio-Malaba-Malakisi basin is a transboundary river basin, dominated by farming communities mainly relying on rain-fed agriculture for their livelihood. However, over the recent past, the basin has experienced an increase in human population (Roussel, 2012) leading to unsustainable land subdivision and intensification of land use activities. As a result, more pressure has been exerted on the limited land resource leading to unplanned land use activities with unpredictable outcomes. Consequently, agricultural activities have expanded in to marginal lands including steep slopes of Mt. Elgon forest leading to massive soil erosion, land degradation and sedimentation on Rivers Sio, Malaba and Malakisi (Karamage et al., 2017). These changes pose a direct threat on the livelihoods of the basin community and the environment overall. An urgent and sustainable solution to the prevailing land management problems is therefore required that will support transboundary land use planning and policy in the area.

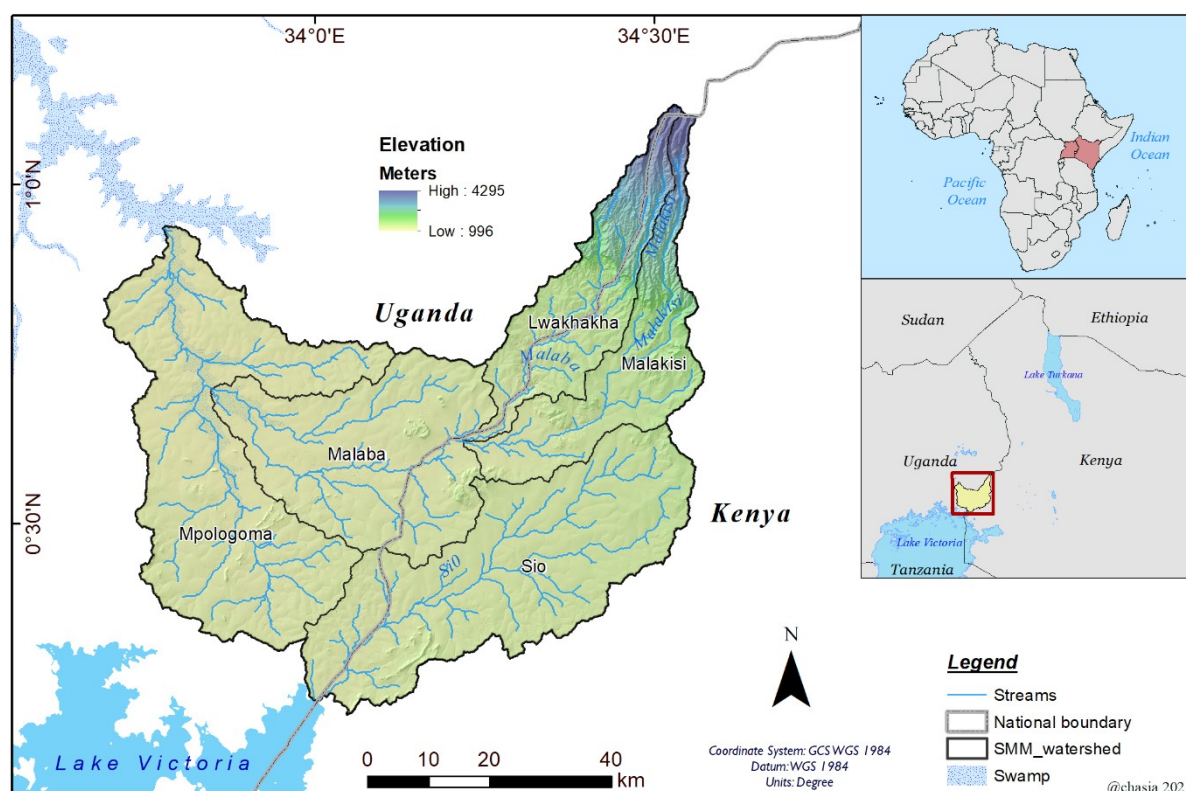


Figure 1. The location of the Sio-Malaba-Malakisi water catchment area between Kenya and Uganda

## 2.2 Data Status and Methods

### 2.2.1 Model Data Requirements

The data, their sources and applications important to define the land cover change driving factors and subsequent simulation of the future spatial patterns of land use/cover types of the basin are provided in Table 1. The datasets can be summarized as climatic (temperature and rainfall), physiographic (altitude, slope, aspect), soil chemical properties i.e., pH, CEC, SOC), socio-economic i.e., population density, literacy levels), and initial land-use map for the period of 2017 previously derived through consistent classification of Landsat 8 satellite data<sup>†</sup>. Another land-use map for 2018 representing “reality” was used for validating model results after the initial simulation run.

Table 1. Data requirements and applications for simulating LULC for SMM basin

Data	Source	Format	Application
Cultivated crops	Field survey (April – July, 2017)	Questionnaire	Total area under different crop

<sup>†</sup>

			category, distribution and yield
Farm inputs	Field survey (April – July, 2017)	Questionnaire	Crop-yield estimation
Literacy level	National Bureau of Statistics	Text files	Proxy for land use change driving factors
Land-use cover maps <sup>‡</sup>	Unites States Geological Survey ( <a href="https://earthexplorer.usgs.gov/">https://earthexplorer.usgs.gov/</a> )	Raster (GeoTIFF)	For simulating land use change and validation
Demographic data	National Bureau of Statistics	Text files	Simulation for all scenarios
Altitude	Digital elevation model (DEM – 90 m)	Raster (GeoTIFF)	Effect of relief on land-use/cover
Slope (degree)	Digital elevation model (DEM – 90 m)	Raster (GeoTIFF)	Effect of slope on land-use/cover
Aspect	Digital elevation model (DEM – 90 m)	Raster (GeoTIFF)	Effect of aspect on land-use/cover
Proximity to roads (trunk, primary and secondary class)	Open street map roads. Distance calculated using Euclidean distance function ( <a href="https://download.geofabrik.de/">https://download.geofabrik.de/</a> )	Raster (GeoTIFF)	Effect of distance to roads on land use type (1 Km)
Proximity to rivers	DEM. Distance calculated using Euclidean distance function	Raster (GeoTIFF)	Effect of distance to rives on land use type (buffer dist. 1 Km)
Proximity to major towns	Open street map towns. Distance calculated using Euclidean distance function	Raster (GeoTIFF)	Effect of distance to major towns on land use type (buffer dist. 5 km)
Erosion and deposition	Calculation of erosion and deposition from RUSLE parameters	Raster grid	Simulation of erosion effect on LULC
Annual average temperature	WorldClim (30 seconds/~1Km)	Raster (GeoTIFF)	Simulation of temperature effect of on LULC pattern
Annual average precipitation (mm)	WorldClim (30 seconds/~1Km)	Raster (GeoTIFF)	Simulation of precipitation effect of on LULC pattern
Soil cation exchange capacity in mmol(c)/kg	Soil Grids (250x250m)	Raster (GeoTIFF)	Simulation of SCE on vegetation cover and pattern
Soil organic carbon in dg/kg	Soil Grids (250x250m)	Raster (GeoTIFF)	Simulation of SOC on vegetation cover and pattern
pH water in soil	Soil Grids (250x250m)	Raster (GeoTIFF)	Simulation of pH on vegetation cover and pattern

The input layers for simulation i.e., all driving factors and the initial land cover map of the study, were initially projected to the same coordinate reference system (WGS 1984 - UTM Zone 36N) of the area and then resampled to 250x250m spatial resolution considering the large size of the basin and data availability (P. Verburg & Veldkamp, 2002). Thereafter, the layers were converted to ASCII file format, as required by CLUE-S, each with the same number of rows, columns and extent similar to the initial land-use map layer of 2017. Tabular data from questionnaires and reports were vectorized in a Geographic Information Systems (GIS) (P. Verburg & Veldkamp, 2002) and later interpolated into a raster grid using the inverse distance weighted method (Luo et al., 2010) .

## 2.3 Identification of Land Cover Change Driving Factors

<sup>‡</sup> This dataset was previously classified and the manuscript from this work is under review

The spatial representations of the potential land cover change driving factors in the study basin are provided in Figure 2. Considering the importance of agriculture in the study area, the identification of biophysical drivers of change was done by evaluating the strength of relationship between the potential driving factors and spatial patterns of land use types against classified historical land cover maps of the study for the period 1985, 1995 and 2008. The use of exploratory regression analysis (Braun & Oswald, 2011) produced the highest adjusted R<sup>2</sup> value of 0.85 (85%) for all land cover classes from combined soil chemical properties, topographical factors and climatic variables. Population density on the other hand produced an adjusted R<sup>2</sup> value of 0.78. Other underlying proximate causes of land cover change i.e., socio-economic factors like literacy levels of the household head and per capita income were selected using questionnaires and interviews sessions conducted between May – July 2017, and evaluated as potential proxies to land-cover change in the study (Briassoulis, 2019; Veldkamp & Verburg, 2004).



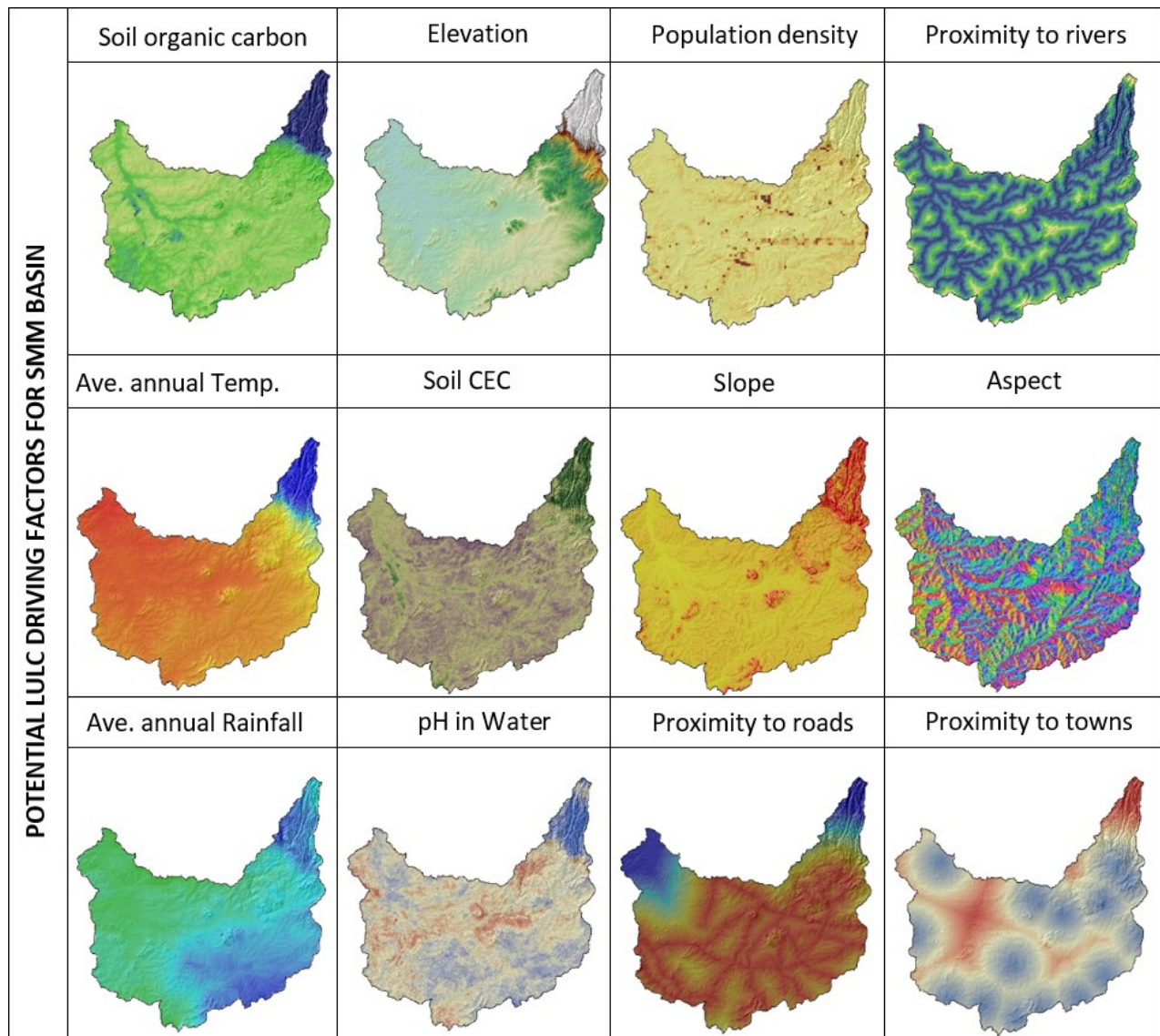


Figure 2. Selected biophysical and socio-economic potential land-use/cover driving factors for model simulation

## 2.4 Modelling Future Land-use –Land-cover Scenarios

### 2.4.1 Description of the CLUE-S Model

For this study, the Conversion of Land Use and its Effects at Small regional extent (CLUE-S) model was applied (Verburg *et al.*, 2002; Verburg & Overmars, 2007). The model is an integrated, spatially explicit, dynamic and multi-scale modelling framework developed at Wageningen University to model land-use change trajectories and processes that determine land-cover patterns at local to regional scales (Briassoulis, 2019; Verburg & Overmars, 2009). The model is composed of two modules namely: (i) a non-spatial demand module used to compute the cumulative area change in LULC and, (ii) a spatially explicit allocation module used to allocate projected demands

in LULC to cell grids based on location characteristics, land-use transition sequences and demand (*Manual for the CLUE-Kenya application*, 2005; Peter H. Verburg et al., 2002). The contribution of potential drivers (herein known as Explanatory Variables) of land-use change are normally estimated using empirical analytical methods (outside the model), where potential driving factors are determined using either the local knowledge of the area or theories of factors of land-use change (D. & A., 1998; Lambin et al., 2001). Simulation using the model requires definitions of land requirements, spatial policies and restrictions, conversion elasticity and land use conversion sequences. In this study, the variables were defined as follows:

#### *(a) Land Requirements*

The land requirement files were prepared through simple trend extrapolation in land use change over the recent past into the near future (P. Verburg & Schulp, 2005; Peter H. Verburg et al., 2002). The trends were corrected for changes in population growth using population projection data from the Kenya National Bureau of Statistics (<https://www.knbs.or.ke/>) and the Uganda National Bureau of Statistics (<https://www.ubos.org/>). Three scenarios were explored in the study based on historical trends in the basin, and their overall impact on local hydrology for future assessment of effects on soil erosion and degradation processes.

First was the *Agri-based Scenario with protection* which explored possible land-use configurations and trajectories following two possibilities: The first explored a situation where the amount of annual rainfall received across the basin remains constant and sufficient enough to support crop growth over the modelling period. In this case, it is assumed that the agricultural land would expand into fallow and open fields with conditions suitable for agriculture. However, due to land-use policy protecting zones of ecological importance i.e., wetlands and natural forest, pixels representing such areas were constrained in the model from changing to cropland. In the second *Agri-based scenario without protection*, cropland areas would expand and occupy neighboring wetland areas capable of supporting rice cultivation. This scenario assumes lack of enforcement of existing land-use regulations leading to encroachment into wetlands. In addition, an increase in commodity prices for rice and human population would be additional driving forces for this conversion.

In the *Afforestation scenario*, the area covered by mixed forest class would increase as a result of public education and the implementation of afforestation programs by public and local private organizations aimed at reducing the rate of land degradation and massive soil erosion. In this scenario, areas previously under open land category would be converted to mixed forest. It is

assumed that the rate of population growth would remain stable over the modelling period and communities living in SMM basin would appreciate the benefits of soil and environmental conservation.

### *(b) Spatial Policies and Restrictions*

Spatial policies restrictions defined areas where change was allowed and areas under government protection. In this study, we experimented with two scenarios. The first scenario represented status quo in which existing policies restricted the conversion of protected areas i.e., forest reserve, wetlands and catchments area to other land-use types. In the second scenario, a section of protected land was converted to other land use types if they met certain set conditions i.e., forest land with fertile soil and favorable climate was converted to agricultural land.

### *(c) Conversion Elasticities*

Land use types were allowed to change from one state to another based on their elasticity. Lu types with high capital investment or irreversible impact on the environment were not allowed to easily change (Table 2). A dimensionless factor representing relative elasticity to conversation was used ranging from 0-easy conversion to 1- irreversible change (Kucsicsa et al., 2019; P.H. Verburg & Overmars, 2007). Areas with permanent structures i.e., urban centers, tree cover and wetlands under protected area were assigned high elasticity values (0.7 – 0.9) limiting their conversion to other land use types. Cropland and open soils on the other hand were assigned low values (0 – 0.4).

*Table 2. Land use conversion elasticities for SMM catchment*

<b>Land-use/cover class</b>	<b>Elasticity</b>
Mixed forest	0.9
Permanent wetland	0.8
Open land/field	0.1
Built-up	1.0
Water	1.0
Open shrubland	0.7
Barren	1.0
Cropland and pasture	0.2

### *(d) Land-use Conversion Sequence*

The conversion sequence file outlines land-use/cover changes allowed and conversions that are not possible. Possible conversions are normally a function of location characteristic defined in equation 1 (P. Verburg et al., 2005).

$$R_{ki} = a_k X_{1i} + b_k X_{2i} + \dots (1)$$

Where  $R$  is the preference to devote location  $i$  to land use type  $k$ .  $X_{1,2}, \dots$  are biophysical and socio-economic characteristics of the location  $i$  and  $a_k$  and  $b_k$  represents the relative impact of these characteristics on the preference of land use type  $K$ . The logit model (Judex & Menz, 2006; Peter H. Verburg et al., 2002) was also used to relate probabilities of LULC allocations with biophysical and socio-economic location characteristics following:

$$\log \left\{ \frac{P_i}{1 - P_i} \right\} = \beta_0 + \beta_1 X_{1,i} + \beta_2 X_{2,i} \dots \beta_n X_{n,i} (2)$$

Where  $P_i$  is the probability of a grid cell for the occurrence of the considered land use type on location  $i$  and the  $X$ 's are the location factors. The coefficients ( $\beta$ ) were estimated using logistic regression using the actual land use pattern as dependent variable (Schneider & Gil Pontius, 2001; P. Verburg & Schulp, 2005).

## 2.5 The Modelling Approach Employed.

The model was parameterized using thirteen independent variables for the regression equation with most variables. The initial model run allowed changes in all land-use classes without a constraining restriction file layer in place. Conversion elasticities were initially set to 0.1, which made changes in all the classes possible. After twenty model runs, elasticity values that provided the most reliable results were 1.0, 0.9, 0.7, 0.8, 0.2, 1.0, 1.0, and 0.1 for barren, mixed forest, open bushland, permanent wetland, cropland and pasture, built-up, water and open land/field respectively. The output map was compared to the 2018 land-cover map used for calibration to assess the level of agreement (Behera & Behera, 2020). The maps of simulated future change in LULC were validated by cross-tabulating each class against the 2019 land use map. The degree of agreement between the two maps was measured to determine the accuracy of the results (Schneider & Gil Pontius, 2001).

## 3 Results

### 3.1 Importance of Driving Factors for dynamic LULC classes

A logistic regression analysis was carried out to determine the importance of each biophysical and socioeconomic factors that influence location and spatial patterns of LULC in SMM. The ROC values obtained for the mixed forest, permanent wetland, cropland and pasture and built-up classes ranged between 0.6 – 0.7 (Table 3) indicating the results are statistically better than random (Gil Pontius Jr & Schneider, 2001). Higher ROC values were noted among the cropland (0.6) and mixed forest (0.7) classes (Fig.3) indicating a strong correlation between these land cover classes and the selected driving factors against each LULC class. Generally, given the spatial dynamic nature of cropland and pasture, more driving factors were included in the regression equation to help explain the spatial distribution of cropland and pasture class across the basin. Proximity to major roads, rivers and towns did not show significant influence on the spatial patterns of land use classes in the study area. However, soil chemical properties and climatic variables strongly influence spatial distribution of different crop types. Coffee and tea for instance, are found in high altitude areas in the basin while grains and leguminous crops were found well distributed across the basin.

*Table 3. Beta values for regression results of spatial distribution of land use in SMM basin*

<i>Driver</i>	<u>Mixed forest</u>		<u>Permanent wetland</u>		<u>Cropland and pasture</u>		<u>Built-up</u>		<u>Open bushland</u>	
	<i>Beta</i>	<i>Exp(B)</i>	<i>Beta</i>	<i>Exp(B)</i>	<i>Beta</i>	<i>Exp(B)</i>	<i>Beta</i>	<i>Exp(B)</i>	<i>Beta</i>	<i>Exp(B)</i>
Constant	-8.719		1.072		-1.300		-6.083		-2.393	
Elevation	0.001	1.001	0.000	1.000	0.000	0.999	0.000	1.000	-0.001	0.999
Slope	0.015	1.015	-0.002	0.998	-0.028	0.972	0.034	1.034	0.000	1.000
Aspect	0.000	1.000	0.000	1.000	0.000	1.000	0.000	1.000	0.000	1.000
Erosion/deposition	0.004	1.004	-0.004	0.996	-0.003	0.997	0.005	1.005	0.001	1.001
Ave. precipitation (p.a)	0.002	1.002	0.000	1.000	0.000	1.000	0.000	1.000	0.004	1.004
Ave. temperature (p.a)	0.003	1.003	0.025	1.025	0.015	1.015	0.002	1.002	0.023	1.023
Distance to stream	0.000	1.000	0.000	1.000	0.000	1.000	0.000	1.000	0.000	1.000
Distance to road	0.000	1.000	-0.001	0.999	0.000	1.000	0.000	1.000	-0.001	0.999
Distance to town	0.000	1.000	0.000	1.000	0.000	1.000	0.000	1.000	0.000	1.000
Population density	0.000	1.000	0.000	1.000	0.000	1.000	0.000	1.000	0.000	1.000
Soil pH	-0.015	0.985	0.091	1.096	0.027	1.028	0.38	1.039	-0.004	0.996
Soil cation exchange capacity	0.016	1.016	0.035	1.035	-0.019	0.981	0.001	1.001	-0.001	0.999
Soil organic carbon	0.023	1.023	-0.013	0.987	-0.006	0.994	-0.001	0.999	0.001	1.001
ROC value	0.698		0.580		0.612		0.578		0.597	

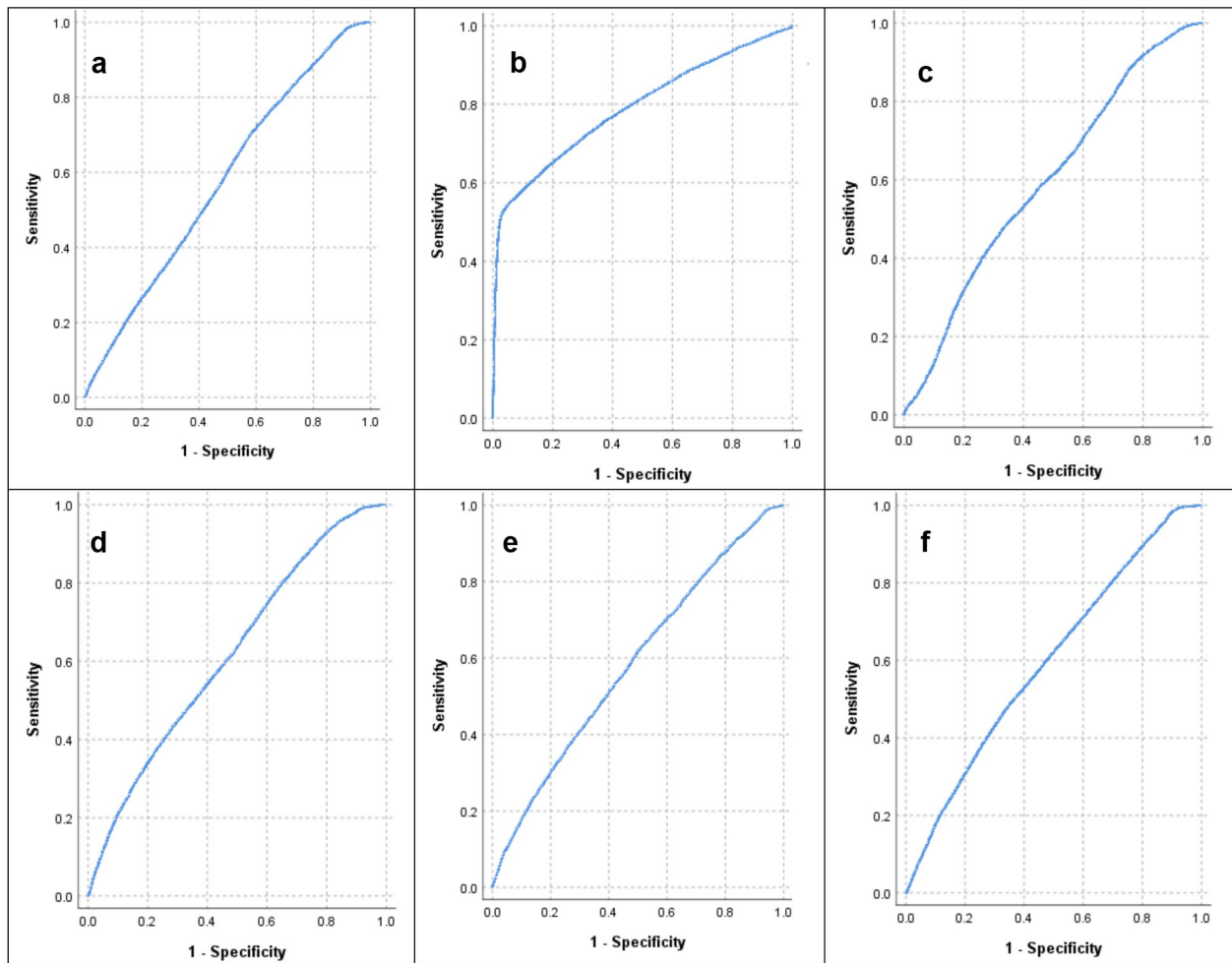


*Figure 3. Sensitivity analysis for (a) cropland and pasture, (b) mixed forest, (c) open bushland, (d) permanent wetland, (e) built-up, (f) open field. The area under the curve represents the ROC values.*

### 3.2 Validation against Historical Land cover states

Historical land use maps for Sio-Malaba-Malakisi basin were available which made the validation of the CLUE-S model performance possible. Model simulations were initialized in 2008 and thereafter a comparison between model results and actual land use changes was made. Eight land use/cover types were simulated for SMM basin (Fig. 4). The most important land-use/cover types were mixed forest, permanent wetland, cropland and pasture, open bushland, built-up and open fields. During the simulation, the barren and water cover types remained static over the modeling period. The Kappa statistic (Manakos & Braun, 2014) was used to evaluate the models ability to replicate statistic was used to evaluate the model's ability to replicate reality and the location of land cover classes(Pontius & Neeti, 2010). The model recorded overall accuracy of 85.7% and a Kappa coefficient of 0.78 for the eight simulated classes. Built-up areas were exaggerated by 10%

due to a limited number of driving factors available in the model. However, barren and water areas produced user's accuracies of 83.6% and 86.3% respectively indicating the model's ability to replicate these classes.

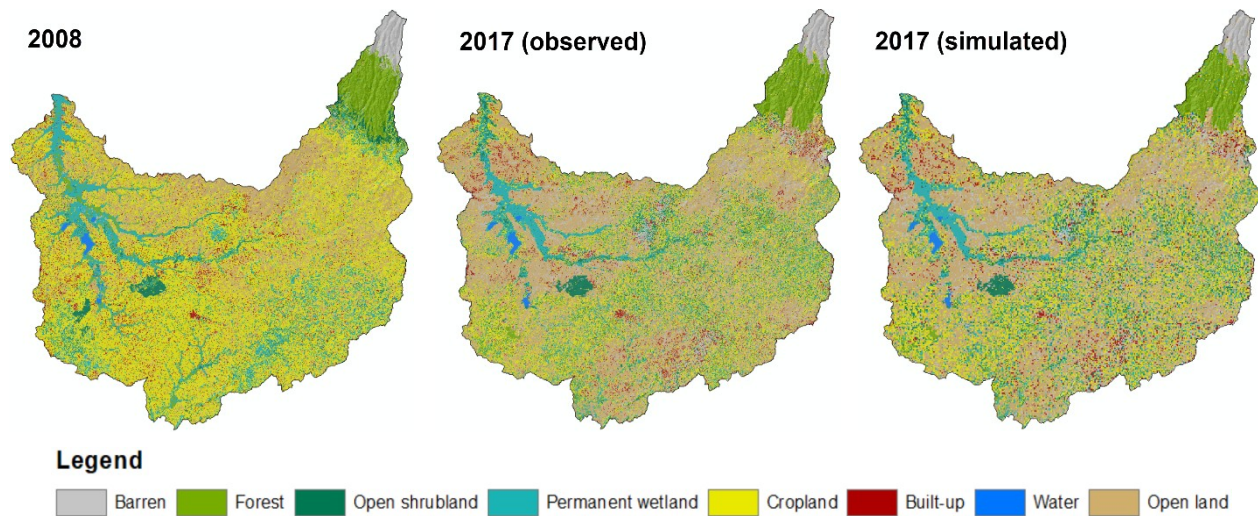


Figure 4. Land use situation in the Sio-Malaba-Malakisi basin in 2008 and 2017 and simulated land use in 2017. The study area covers a total extent of 5200km<sup>2</sup>. Each grid-cell is 250m.

### 3.3 Projected land-use cover for the period 2017 - 2047

Table 5 provides an illustration of changes in land cover classes under different scenarios. The area in hectares for land cover classes for the starting period in the model are represented under the current state column. In 2017, open fields occupied the largest land cover size in the basin at 40.1%. Cropland and pasture came second occupying 22.7%, while mixed forest, open shrubland, permanent wetland and water occupied 6.8%, 6.7%, 9.2%, 0.3% respectively (Fig. 6-So).

#### 3.3.1 Scenario 1 – Projected LULC Change for Afforestation Scenario

The afforestation scenario explored changes in LULC in SMM over a continuous period of thirty years when afforestation programs are enhanced across the basin to control soil erosion and vegetation cover. This scenario assumes availability of land and other incentives to promote the growth of both exotic and indigenous trees by the local community. In addition, forested areas previously lost to cropland in areas near Busitema forest and the southern edges of Mt. Elgon forest would be reclaimed back. In this scenario therefore, 64,279ha of mixed forest and 69,438ha of open bush were recovered, representing a 54.7% and 50% growth respectively. This involved conversion of previously open land and fallow areas capable of supporting trees (Fig. 5). On the edges of Mt. Elgon forest, this involved conversion of cropland areas in Chepyuk settlement



scheme which originally were under natural forest in 1986. Other regions that experienced significant change include Busitema forest in Uganda and its surroundings areas which were encroached by neighboring farming communities.

### 3.3.2 Scenario 2 – Projected LULC Change for Intense Agriculture Scenario

In the intense agriculture with no restrictions for expansion scenario ( $S_2$ ), cropland and pasture were projected to increase by 255,581ha and occupy up to 78.3% of the total basin area (Table 4) representing a 49.6% growth from the base year. This involved conversion of open bushland and open land and areas under permanent wetland to cropland and pasture (Fig. 5-S2). Improvement in weather conditions, access to farm inputs like fertilizer and improvements in commodity prices especially rice, were assumed to be key driving of change under this scenario.

Table 4. Percentage change in different land-use/cover classes under different scenarios

LULC	2017	2047		
	$S0$ (ha)	$S1$ (ha)	$S2$ (ha)	$S3$ (ha)
Water (Wt)	7781	7,325	7,169	7,169
Permanent wetland (Pw)	50,294	56,088	0	56,244
Open land (Ol)	206,700	0	0	0
Built-up (Bu)	17,475	22,088	22,088	22,088
Open bushland	34,719	104,157	0	0
Mixed forest (Mf)	35,188	99,467	67,688	67,688
Barren (Br)	15,263	14,894	14,894	14,894
Cropland and pasture (Cp)	147,580	210,981	403,161	346,917
<i>Perc. change</i>		<i>54.7%</i>	<i>78.3%</i>	<i>61.7%</i>



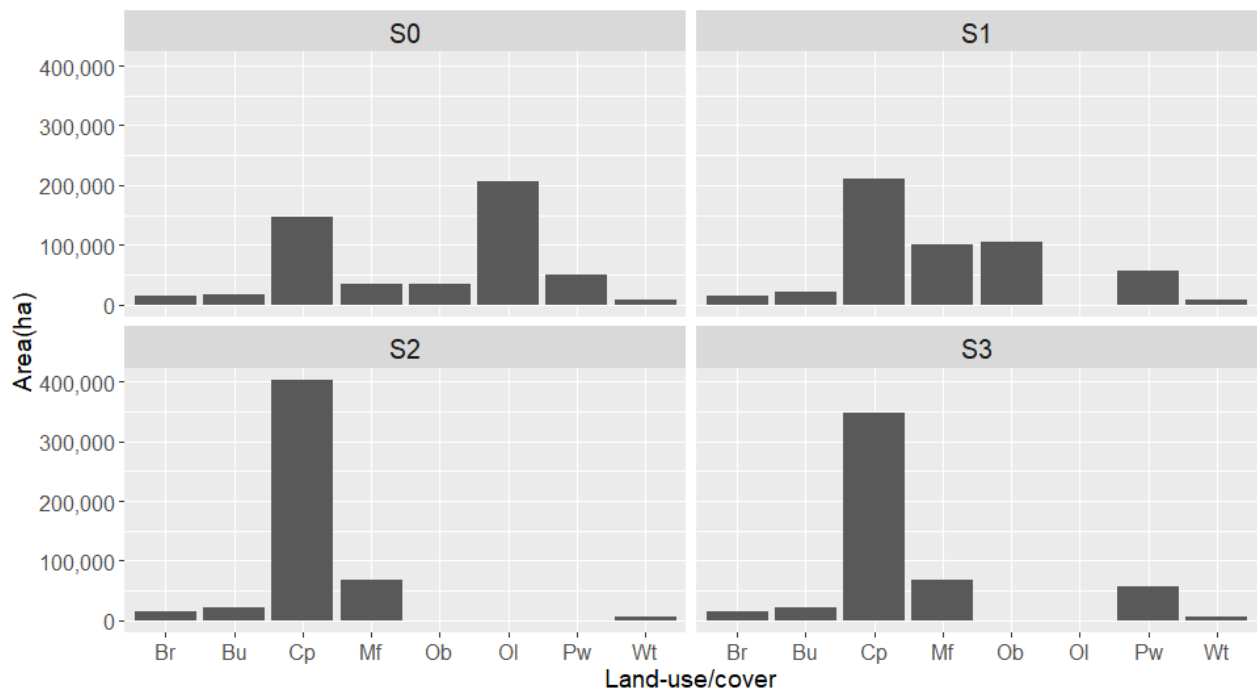


Figure 5. Land-use/cover change trajectories under afforestation(S1); Intense agriculture under no restrictions(S2) and agriculture expansion under protected wetland(S3). S0-current LULC state.

In figure 6-S2, areas that were previously under permanent wetland and open land areas in 2017 were converted to cropland as a result of the expansion and intensification of agricultural activities. The areas under mixed forest category were not significantly affected by this expansion.

### 3.3.3 Scenario 3 – Projected LULC Change for intense Agriculture under Protected Wetlands

The third scenario explored the land-cover trajectories in the basin when permanent wetlands areas are protected from encroachment agricultural activities. These changes were constrained in the model by reducing conversion elasticities of permanent wetlands and mixed forest to 0.7 and 0.9 respectively. However, the model still allowed some changes to occur in areas that met the conversion criteria. Consequently, cropland and pasture increase by 199,337ha representing a 74% increase from the initial modeling period. The constraint imposed in the model that reduced the elasticity value of permanent wetland to 0.8, increased the conversion cost, subsequently leading to the recovery of approximately 12% (5,950ha) of the permanent wetland area. However, all available land under open land and open bushland category were converted to cropland and pasture. Overall, areas under barren and water covers (Fig. 6-S0) remained static over the modelling period with a constraining elasticity value of 1.0. This is because barren areas were located in very high-altitude zones in the basin and are mainly covered by rock outcrops. Areas

under water on the other hand, were treated as protected areas with no conversion allowed. In addition, such land cover types could not support agricultural activities.

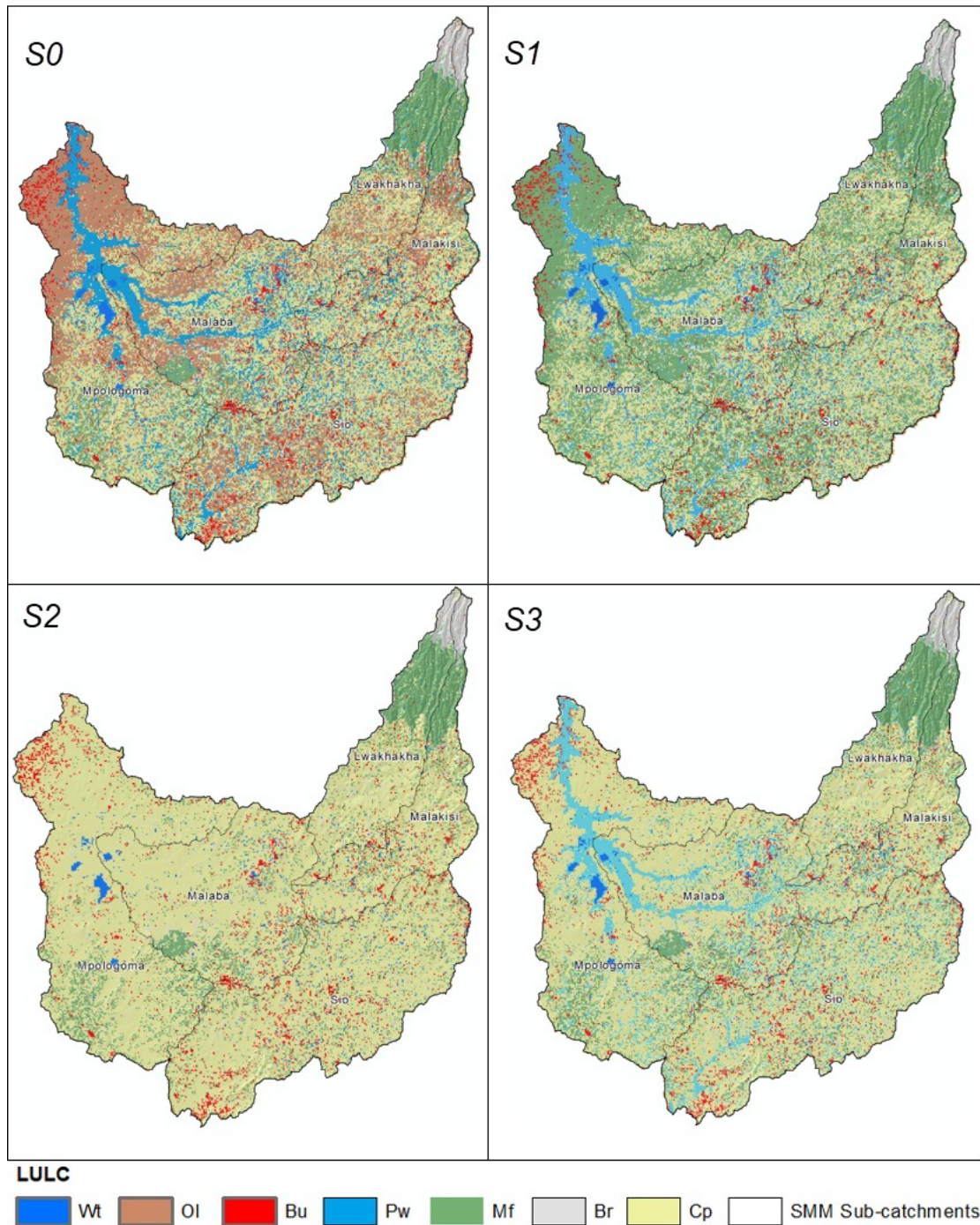


Figure 6. Model simulation results. **S0** – Land-use situation at the start of the simulations in 2017; **S1**, simulation results for the Afforestation scenario in 2047; **S2**, simulations result for 2047 under intense agriculture conditions; **S3**, simulation results for 2047 under the intense agriculture under protected land

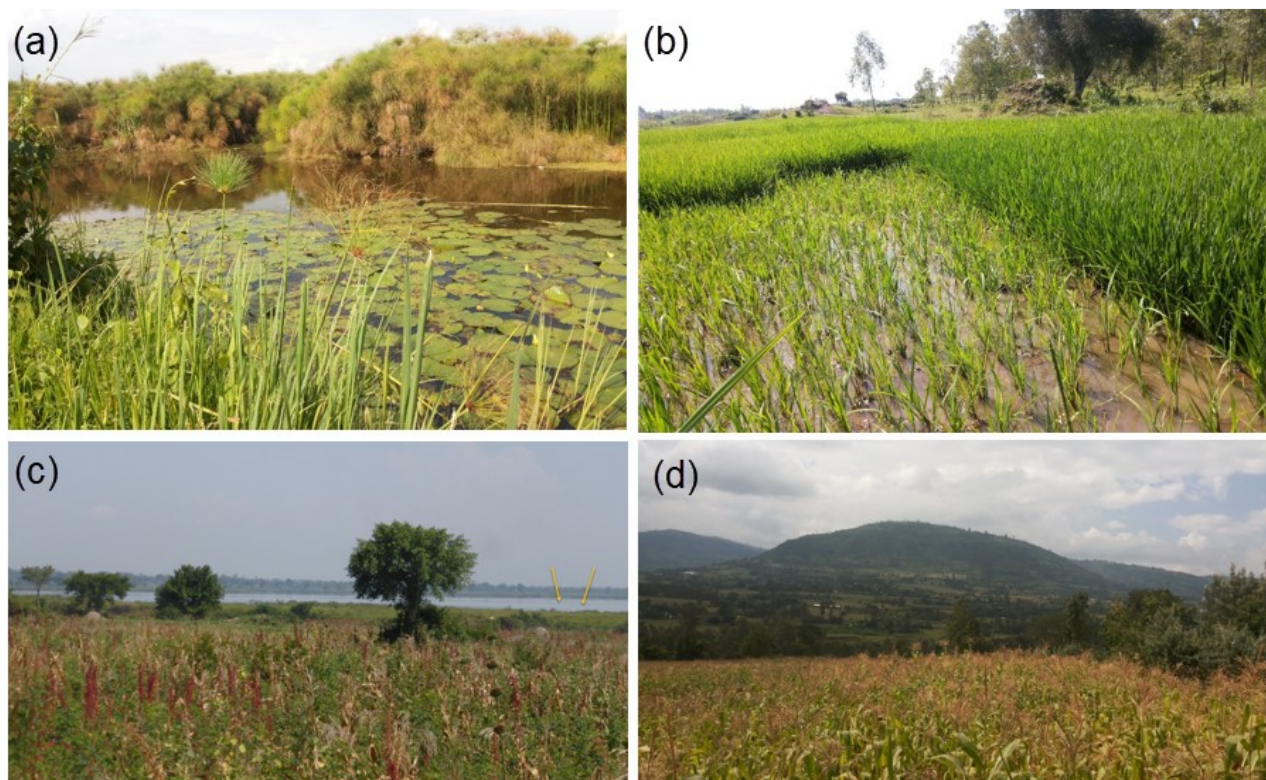


Figure 7. Land cover types in SMM basin - **a)** Areas of permanent wetland, **b)** Cropland (rice) cultivation on sections of wetlands, **c)** Areas covered by permanent water (yellow arrows), **d)** Cultivation of food crops. Photos by Chasia and Wemer

## 4 Discussion

### 4.1 Accuracy assessment

Table 5 illustrates the cross-tabulation output for three scenarios over five model runs against the reality map. The false-positive column represents pixels considered to have changed in the modeled scenario output but in reality, the change didn't occur. True-positive column on the other hand represents pixels that changed in both reality and modeled scenario maps (Gil Pontius Jr & Schneider, 2001). The ROC values for the afforestation scenario ( $S_1$ ), intense agriculture( $S_2$ ), and agriculture under protected wetlands scenario( $S_3$ ), were 50%, 65% and 70% respectively.

Table 5. Cross tabulation between grid cells in a reality map and suitability map for 5 scenarios of afforestation, unrestricted intense agriculture, and intense agriculture within wetland protection

Scenario suitability	Reality		Cumulative Reality			Scenario statistics		
	Change	No-change	Change	No-change	Change	Correct	False positive	True positive

S1								
1	0.1	0.1	0.1	0.1	12.3	99.9	11.1	6.7
2	0.6	0.4	0.7	0.5	65.7	99.5	55.6	46.7
3	0.2	0.2	0.9	0.7	21.6	99.3	77.8	60.0
4	0.4	0.1	1.3	0.8	2.1	99.2	88.9	86.7
5	0.2	0.1	1.5	0.9	2.4	99.1	100	100
S2								
1	0.2	0.5	1.7	1.4	3.1	3.4	41.2	43.6
2	0.4	0.7	2.1	2.1	4.2	97.9	61.8	53.8
3	0.3	0.3	2.4	2.4	4.8	97.6	70.6	61.5
4	0.9	0.4	3.3	2.8	6.1	97.2	82.4	84.6
5	0.6	0.6	3.9	3.4	7.3	96.6	100	100
S3								
1	0.4	0.2	4.3	3.6	7.9	17.4	20.7	81.1
2	0.3	0.3	4.6	3.9	8.5	96.1	22.4	86.8
3	0.4	0.7	5.0	4.6	9.6	95.4	26.4	94.3
4	0.2	0.5	5.2	5.1	10.3	94.9	29.3	98.1
5	0.1	12.3	5.3	17.4	22.7	82.6	100	100

Generally, there was a low agreement (ROC 50%) between afforestation scenario and the reality map. However, intense agriculture and agriculture under protected wetlands, recorded relatively higher ROC values of 65% and 70% respectively, indicating a moderate to strong agreement between the modeled scenarios and the reality map. The lower ROC values for the afforestation scenario is attributed to the low elasticity values for open land and cropland classes which were easily converted to the mixed forest class. Among the twelve potential drivers analyzed in the study against the land-use/cover classes, distance to streams, road and towns had little to no influence on the location of land use activities (Fig. 8). However, chemical soil properties of pH, organic carbon content, and the cation exchange capacity had a significant influence on cropland and pasture, mixed forest class and permanent wetlands classes. The nature of soil property which determines agricultural productivity was considered important in SMM basin since majority of the community members there practice agriculture. The higher pH values for the permanent wetland class could be attributed to nutrient loads from fertilizers washed off the farms and transported by surface run-off to nearby rivers draining their water into the wetlands.



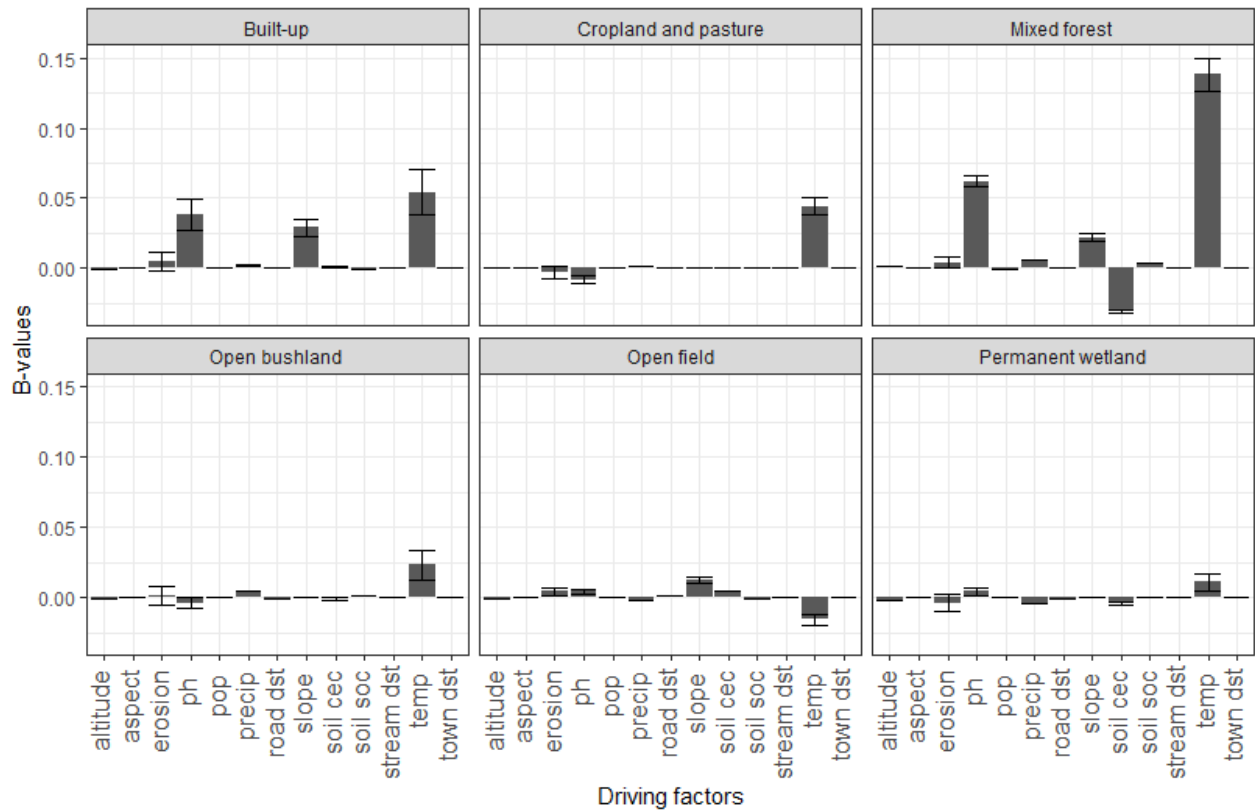


Figure 8. Beta values from regression analysis indicating importance of biophysical and socio-economic driving factors used for LULC classes

The afforestation scenario in the study presented an optimistic view of land management in the basin following years of intensive human activities leading to land degradation. In this scenario, areas that were originally under natural forests were reclaimed while any available open land area capable of supporting tree plantations would be used to increase the percentage forest cover. The scenario envisioned a situation where incentives for land conservation outweighed short-term benefits that normally lead to soil erosion and land degradation. Scenario two under intense agriculture presented a situation where farmlands extend into protected areas including wetlands and open fields capable of supporting agriculture. A steady increase in human population and an improvement in market prices, promoted the growth of rice in sections of wetlands capable of supporting rice cultivation. Other factors that promote crop cultivation include access to farm inputs like fertilizers and farming technology. The third scenario projected a future characterized by expansion in agriculture but only in areas not restricted by government policy like protected areas. In this scenario therefore, less than 0.4% of the permanent wetland area would be converted to cropland and pasture.

In conclusion, scenarios used in this study were based on local knowledge and analysis of historical land-cover data applying trend extrapolation technique. Future patterns in LULC in the

study were mainly influenced by biophysical variables which are known to control certain conditions like suitable areas for plant growth i.e., temperature regime, precipitation and soil fertility. However, access to modern technology, farmers training and use of fertilizers has enabled farmers to overcome some of the biophysical limiting factors that control land use activities. Consequently, this study considers socio-economic drivers playing an important role in land use decisions and model performance in the basin.

## Acknowledgements

This work was supported by funds from the Austrian Development Cooperation through the Austrian Partnership Programme in Higher Education and Research for Development (APPEAR)

**Conflict of interest Statement:** As authors, we confirm that there is no potential conflict of interest

## References

- Alemayehu, T., Griensven, A. van, Senay, G. B., & Bauwens, W. (2017). Evapotranspiration Mapping in a Heterogeneous Landscape Using Remote Sensing and Global Weather Datasets: Application to the Mara Basin, East Africa. *Remote Sensing*, 9(4), 390. <https://doi.org/10.3390/rs9040390>
- Ban, Y., Gong, P., & Giri, C. (2015). Global land cover mapping using Earth observation satellite data: Recent progresses and challenges. *ISPRS Journal of Photogrammetry and Remote Sensing*, 103, 1–6. <https://doi.org/10.1016/j.isprsjprs.2015.01.001>
- Behera, N. K., & Behera, M. D. (2020). Predicting land use and land cover scenario in Indian national river basin: the Ganga. *Tropical Ecology*, 61(1), 51–64. <https://doi.org/10.1007/s42965-020-00073-x>
- Braun, M. T., & Oswald, F. L. (2011). Exploratory regression analysis: A tool for selecting models and determining predictor importance. In *Behavior Research Methods* (Vol. 43, Issue 2, pp. 331–339). Springer. <https://doi.org/10.3758/s13428-010-0046-8>
- Briassoulis, H. (2019). *Analysis of land use change: theoretical and modeling approaches*. Regional Research Institute, West Virginia University.
- Camberlin, P., & Okoola, R. E. (2003). The onset and cessation of the “long rains” in eastern Africa and their interannual variability. *Theoretical and Applied Climatology*, 75(1–2), 43–

54. <https://doi.org/10.1007/s00704-002-0721-5>

- Cegielska, K., Noszczyk, T., Kukulska, A., Szylar, M., Hernik, J., Dixon-Gough, R., Jombach, S., Valánszki, I., & Filepné Kovács, K. (2018). Land use and land cover changes in post-socialist countries: Some observations from Hungary and Poland. *Land Use Policy*, 78, 1–18. <https://doi.org/10.1016/j.landusepol.2018.06.017>
- Chaudhuri, G., & Clarke, K. C. (2013). The SLEUTH Land Use Change Model: A Review. In *The International Journal of Environmental Resources Research* (Vol. 1, Issue 1). Gorgan University of Agricultural Sciences and Natural Resources. <https://doi.org/10.22069/IJERR.2013.1688>
- Chen, C., Park, T., Wang, X., Piao, S., Xu, B., Chaturvedi, R. K., Fuchs, R., Brovkin, V., Ciais, P., Fensholt, R., Tømmervik, H., Bala, G., Zhu, Z., Nemani, R. R., & Myneni, R. B. (2019). China and India lead in greening of the world through land-use management. *Nature Sustainability*, 2(2), 122–129. <https://doi.org/10.1038/s41893-019-0220-7>
- Claessens, L., Schoorl, J. M., Verburg, P. H., Geraedts, L., & Veldkamp, A. (2009). Modelling interactions and feedback mechanisms between land use change and landscape processes. *Agriculture, Ecosystems & Environment*, 129(1–3), 157–170. <https://doi.org/10.1016/j.agee.2008.08.008>
- Congalton, R., Gu, J., Yadav, K., Thenkabail, P., & Ozdogan, M. (2014). Global Land Cover Mapping: A Review and Uncertainty Analysis. *Remote Sensing*, 6(12), 12070–12093. <https://doi.org/10.3390/rs61212070>
- D., K., & A., A. (1998). Economic models of tropical deforestation: a review. In *Economic models of tropical deforestation: a review*. Center for International Forestry Research (CIFOR). <https://doi.org/10.17528/cifor/000341>
- Du, X., & Huang, Z. (2017). Ecological and environmental effects of land use change in rapid urbanization: The case of hangzhou, China. *Ecological Indicators*, 81, 243–251. <https://doi.org/10.1016/j.ecolind.2017.05.040>
- Duveiller, G., Caporaso, L., Abad-Viñas, R., Perugini, L., Grassi, G., Arneth, A., & Cescatti, A. (2020). Local biophysical effects of land use and land cover change: towards an assessment tool for policy makers. *Land Use Policy*, 91, 104382. <https://doi.org/10.1016/j.landusepol.2019.104382>

- Fayos, C. B. (2002). *Competition over water resources: analysis and mapping of water-related conflicts in the catchment of Lake Naivasha (Kenya)* (Issue February). International Institute for Geoinformation Science and Earth Observation.
- Fetzel, T., Niedertscheider, M., Haberl, H., Krausmann, F., & Erb, K. H. (2016). Patterns and changes of land use and land-use efficiency in Africa 1980–2005: an analysis based on the human appropriation of net primary production framework. *Regional Environmental Change*, 16(5), 1507–1520. <https://doi.org/10.1007/s10113-015-0891-1>
- Foley, J. A., DeFries, R., Asner, G. P., Barford, C., Bonan, G., Carpenter, S. R., Chapin, F. S., Coe, M. T., Daily, G. C., Gibbs, H. K., Helkowski, J. H., Holloway, T., Howard, E. A., Kucharik, C. J., Monfreda, C., Patz, J. A., Prentice, I. C., Ramankutty, N., & Snyder, P. K. (2005). Global consequences of land use. *Science*, 309(5734), 570–574. <https://doi.org/10.1126/science.1111772>
- Gil Pontius Jr, R., & Schneider, L. C. (2001). Land-cover change model validation by an ROC method for the Ipswich watershed, Massachusetts, USA. In *Ecosystems and Environment* (Vol. 85).
- Griscom, H. R., Miller, S. N., Gyedu-Ababio, T., & Sivanpillai, R. (2010). Mapping land cover change of the Luvuvhu catchment, South Africa for environmental modelling. *GeoJournal*, 75(2), 163–173. <https://doi.org/10.1007/s10708-009-9281-x>
- Hartemink, A., & van Keulen, H. (2005). Soil degradation in Sub-Saharan Africa. *Land Use Policy*, 22(1), 1. <https://doi.org/10.1016/j.landusepol.2004.01.001>
- Huang, D., Huang, J., & Liu, T. (2019). Delimiting urban growth boundaries using the CLUE-S model with village administrative boundaries. *Land Use Policy*, 82, 422–435. <https://doi.org/10.1016/j.landusepol.2018.12.028>
- Irwin, E. G., & Geoghegan, J. (2001). Theory, data, methods: Developing spatially explicit economic models of land use change. *Agriculture, Ecosystems and Environment*, 85(1–3), 7–24. [https://doi.org/10.1016/S0167-8809\(01\)00200-6](https://doi.org/10.1016/S0167-8809(01)00200-6)
- Jiang, W., Chen, Z., Lei, X., Jia, K., & Wu, Y. (2015). Simulating urban land use change by incorporating an autologistic regression model into a CLUE-S model. *Journal of Geographical Sciences*, 25(7), 836–850. <https://doi.org/10.1007/s11442-015-1205-8>
- Judex, M., & Menz, G. (2006). Modelling of land-use changes in a West African catchment. *ISPR*



*Archives*, 36(7), 18.

- Karamage, F., Zhang, C., Liu, T., Maganda, A., & Isabwe, A. (2017). Soil Erosion Risk Assessment in Uganda. *Forests*, 8(2), 52. <https://doi.org/10.3390/f8020052>
- Kucsicsa, G., Popovici, E.-A., Bălteanu, D., Grigorescu, I., Dumitraşcu, M., & Mitrică, B. (2019). Future land use/cover changes in Romania: regional simulations based on CLUE-S model and CORINE land cover database. *Landscape and Ecological Engineering*, 15(1), 75–90. <https://doi.org/10.1007/s11355-018-0362-1>
- Lambin, E. F., & Ehrlich, D. (1997). Land-cover changes in Sub-Saharan Africa (1982-1991): Application of a change index based on remotely sensed surface temperature and vegetation indices at a continental scale. *Remote Sensing of Environment*, 61(2), 181–200. [https://doi.org/10.1016/S0034-4257\(97\)00001-1](https://doi.org/10.1016/S0034-4257(97)00001-1)
- Lambin, E. F., Turner, B. L., Geist, H. J., Agbola, S. B., Angelsen, A., Folke, C., Bruce, J. W., Coomes, O. T., Dirzo, R., George, P. S., Homewood, K., Imbernon, J., Leemans, R., Li, X., Moran, E. F., Mortimore, M., Ramakrishnan, P. S., Richards, J. F., Steffen, W., ... Veldkamp, T. A. (2001). *The causes of land-use and land-cover change: moving beyond the myths* (Vol. 11).
- Liping, C., Yujun, S., & Saeed, S. (2018). Monitoring and predicting land use and land cover changes using remote sensing and GIS techniques—A case study of a hilly area, Jiangle, China. *PLoS ONE*, 13(7), 1–23. <http://10.0.5.91/journal.pone.0200493>
- Lone, S. A., & Mayer, I. A. (2019). Geo-spatial analysis of land use/land cover change and its impact on the food security in District Anantnag of Kashmir Valley. *GeoJournal*, 84(3), 785–794. <https://doi.org/10.1007/s10708-018-9891-2>
- Luo, G., Yin, C., Chen, X., Xu, W., & Lu, L. (2010). Combining system dynamic model and CLUE-S model to improve land use scenario analyses at regional scale: A case study of Sangong watershed in Xinjiang, China. *Ecological Complexity*, 7(2), 198–207. <https://doi.org/10.1016/j.ecocom.2010.02.001>
- Maitima, J. M., Mugatha, S. M., Reid, R. S., Gachimbi, L. N., Majule, A., Lyaruu, H., Pomery, D., Mathai, S., & Mugisha, S. (2009). The linkages between land use change, land degradation and biodiversity across East Africa. *African Journal of Agricultural Research*, 3(10), 310–325. <https://doi.org/10.5897/AJEST08.173>

- Manakos, I., & Braun, M. (2014). *Remote Sensing and Digital Image Processing Land Use and Land Cover Mapping in Europe*. [https://doi.org/Manakos, I., & Braun, M. \(n.d.\). Remote Sensing and Digital Image Processing Land Use and Land Cover Mapping in Europe. \(I. Manakos & M. Braun, Eds.\). Springer Science + Business Media. Retrieved from http://www.springer.com/series/6477](https://doi.org/Manakos, I., & Braun, M. (n.d.). Remote Sensing and Digital Image Processing Land Use and Land Cover Mapping in Europe. (I. Manakos & M. Braun, Eds.). Springer Science + Business Media. Retrieved from http://www.springer.com/series/6477)
- Marcos-Martinez, R., Bryan, B. A., Connor, J. D., & King, D. (2017). Agricultural land-use dynamics: Assessing the relative importance of socioeconomic and biophysical drivers for more targeted policy. *Land Use Policy*, 63, 53–66. <https://doi.org/10.1016/j.landusepol.2017.01.011>
- Matthews, R. B., Gilbert, N. G., Roach, A., Polhill, J. G., & Gotts, N. M. (2007). Agent-based land-use models: A review of applications. In *Landscape Ecology* (Vol. 22, Issue 10, pp. 1447–1459). Springer. <https://doi.org/10.1007/s10980-007-9135-1>
- Midekisa, A., Holl, F., Savory, D. J., Andrade-Pacheco, R., Gething, P. W., Bennett, A., & Sturrock, H. J. W. (2017). Mapping land cover change over continental Africa using Landsat and Google Earth Engine cloud computing. *PLoS ONE*, 12(9), 1–15. <https://doi.org/10.1371/journal.pone.0184926>
- Mohammady, M., Moradi, H. R., Zeinivand, H., Temme, A. J. A. M., Yazdani, M. R., & Pourghasemi, H. R. (2018). Modeling and assessing the effects of land use changes on runoff generation with the CLUE-s and WetSpa models. *Theoretical & Applied Climatology*, 133(1–2), 459–471. <http://10.0.3.239/s00704-017-2190-x>
- Newbold, T., Hudson, L. N., Hill, S. L. L., Contu, S., Lysenko, I., Senior, R. A., Börger, L., Bennett, D. J., Choimes, A., Collen, B., Day, J., De Palma, A., Díaz, S., Echeverria-Londoño, S., Edgar, M. J., Feldman, A., Garon, M., Harrison, M. L. K., Alhusseini, T., ... Purvis, A. (2015). Global effects of land use on local terrestrial biodiversity. *Nature*, 520(7545), 45–50. <https://doi.org/10.1038/nature14324>
- Olang, L. O., Kundu, P. M., Ouma, G., & Fürst, J. (2014). Impacts of land cover change scenarios on storm runoff generation: A basis for management of the Nyando Basin, Kenya. *Land Degradation and Development*, 25(3), 267–277. <https://doi.org/10.1002/ldr.2140>
- Ongoma, V., Chen, H., & Omony, G. W. (2018). Variability of extreme weather events over the equatorial East Africa, a case study of rainfall in Kenya and Uganda. *Theoretical and Applied Climatology*, 131(1–2), 295–308. <https://doi.org/10.1007/s00704-016-1973-9>

- Peng, K., Jiang, W., Deng, Y., Liu, Y., Wu, Z., & Chen, Z. (2020). Simulating wetland changes under different scenarios based on integrating the random forest and CLUE-S models: A case study of Wuhan Urban Agglomeration. *Ecological Indicators*, 117, 106671. <https://doi.org/10.1016/j.ecolind.2020.106671>
- Petursson, J. G., Vedeld, P., & Kaboggoza, J. (2011). Transboundary biodiversity management: Institutions, local stakeholders, and protected areas: A case study from Mt. Elgon, Uganda And Kenya. *Society and Natural Resources*, 24(12), 1304–1321. <https://doi.org/10.1080/08941920.2010.540310>
- Pontius, R. G., & Neeti, N. (2010). Uncertainty in the difference between maps of future land change scenarios. *Sustainability Science*, 5(1), 39–50. <https://doi.org/10.1007/s11625-009-0095-z>
- Reed, M. S., & Clokie, M. R. J. (2000). Effects of grazing and cultivation on forest plant communities in Mount Elgon National Park, Uganda. *African Journal of Ecology*, 38(2), 154–162. <https://doi.org/10.1046/j.1365-2028.2000.00234.x>
- Roussel, J.-M. (2012). *Feasibility study and preparation of an integrated watershed management program and investment proposal for Sio-Malaba-Malakisi sub basin* (Issue May). <http://nileis.nilebasin.org>
- Saxena, A., & Jat, M. K. (2019). Capturing heterogeneous urban growth using SLEUTH model. *Remote Sensing Applications: Society and Environment*, 13, 426–434. <https://doi.org/10.1016/j.rsase.2018.12.012>
- Schneider, L. C., & Gil Pontius, R. (2001). Modeling land-use change in the Ipswich watershed, Massachusetts, USA. *Agriculture, Ecosystems and Environment*, 85(1–3), 83–94. [https://doi.org/10.1016/S0167-8809\(01\)00189-X](https://doi.org/10.1016/S0167-8809(01)00189-X)
- Schulp, C. J. E., Levers, C., Kuemmerle, T., Tieskens, K. F., & Verburg, P. H. (2019). Mapping and modelling past and future land use change in Europe's cultural landscapes. *Land Use Policy*, 80, 332–344. <https://doi.org/10.1016/j.landusepol.2018.04.030>
- Schürz, C., Mehdi, B., Kiesel, J., Schulz, K., & Herrnegger, M. (2020). A systematic assessment of uncertainties in large-scale soil loss estimation from different representations of USLE input factors – a case study for Kenya and Uganda. *Hydrology and Earth System Sciences*, 24(9), 4463–4489. <https://doi.org/10.5194/hess-24-4463-2020>

- Song, X.-P., Hansen, M. C., Stehman, S. V., Potapov, P. V., Tyukavina, A., Vermote, E. F., & Townshend, J. R. (2018). Global land change from 1982 to 2016. *Nature*, 560(7720), 639–643. <https://doi.org/10.1038/s41586-018-0411-9>
- Thenkabail, P. S. (2016). *Remote sensing handbook. Volume II, Land resources monitoring, modeling, and mapping with remote sensing: Vol. II*. <https://www.crcpress.com/Land-Resources-Monitoring-Modeling-and-Mapping-with-Remote-Sensing/Thenkabail-PhD/p/book/9781482217957>
- Tizora, P., Le Roux, A., Mans, G., & Cooper, A. K. (2018). Adapting the Dyna-CLUE model for simulating land use and land cover change in the Western Cape Province. *South African Journal of Geomatics*, 7(2), 190. <https://doi.org/10.4314/sajg.v7i2.7>
- UNDP. (2018). *Human Development Indices: 2018 Statistical update Kenya*. [http://hdr.undp.org/sites/all/themes/hdr\\_theme/country-notes/KEN.pdf](http://hdr.undp.org/sites/all/themes/hdr_theme/country-notes/KEN.pdf)
- van Soesbergen, A., & MacArthur Foundation, C. T. (2016). *A REVIEW OF LAND-USE CHANGE MODELS*. [www.unep-wcmc.org](http://www.unep-wcmc.org)
- Vanwalleghe, T., Gómez, J. A., Infante Amate, J., González de Molina, M., Vanderlinden, K., Guzmán, G., Laguna, A., & Giráldez, J. V. (2017). Impact of historical land use and soil management change on soil erosion and agricultural sustainability during the Anthropocene. In *Anthropocene* (Vol. 17, Issue 17). <https://doi.org/10.1016/j.ancene.2017.01.002>
- Veldkamp, A., & Verburg, P. H. (2004). Modelling land use change and environmental impact. *Journal of Environmental Management*, 72(1–2), 1–3. <https://doi.org/10.1016/j.jenvman.2004.04.004>
- Verburg, P., & Schulp, N. (2005). *Manual for the CLUE-Kenya application. June*, 1–54.
- Manual for the CLUE-Kenya application, (2005).
- Verburg, P., Steeg, J. Van De, & Schulp, N. (2005). *Manual for the CLUE-Kenya application. June*, 1–54.
- Verburg, P., & Veldkamp, T. (2002). European Advanced Study Course Modelling Land Use Change 27 October 2002- 2 November 2002. *Environmental Modeling & Assessment, October*. <https://doi.org/10.1007/s00267-002-2630-x>
- Verburg, P.H., & Overmars, K. P. (2007). Dynamic Simulation of Land-Use Change Trajectories

- with the Clue-s Model. In *Modelling Land-Use Change* (Vol. 90, pp. 321–335). Springer Netherlands. [https://doi.org/10.1007/1-4020-5648-6\\_18](https://doi.org/10.1007/1-4020-5648-6_18)
- Verburg, Peter H., Alexander, P., Evans, T., Magliocca, N. R., Malek, Z., Rounsevell, M. DA, & van Vliet, J. (2019). Beyond land cover change: towards a new generation of land use models. *Current Opinion in Environmental Sustainability*, 38, 77–85. <https://doi.org/10.1016/j.cosust.2019.05.002>
- Verburg, Peter H., & Overmars, K. P. (2009). Combining top-down and bottom-up dynamics in land use modeling: exploring the future of abandoned farmlands in Europe with the Dyna-CLUE model. *Landscape Ecology*, 24(9), 1167–1181. <https://doi.org/10.1007/s10980-009-9355-7>
- Verburg, Peter H., Soepboer, W., Veldkamp, A., Limpiada, R., Espaldon, V., & Mastura, S. S. A. (2002). Modeling the spatial dynamics of regional land use: The CLUE-S model. *Environmental Management*, 30(3), 391–405. <https://doi.org/10.1007/s00267-002-2630-x>
- Verburg, Peter H., Schot, P. P., Dijst, M. J., & Veldkamp, A. (2004). *Land use change modelling: current practice and research priorities. 1*, 309–324.
- Waiyasusri, K., Yumuang, S., & Chotpantararat, S. (2016). Monitoring and predicting land use changes in the Huai Thap Salao Watershed area, Uthaitani Province, Thailand, using the CLUE-s model. *Environmental Earth Sciences*, 75(6), 1–16. <https://doi.org/10.1007/s12665-016-5322-1>
- Wang, F., Yuan, X., & Xie, X. (2021). Dynamic change of land use/land cover patterns and driving factors of Nansihu Lake Basin in Shandong Province, China. *Environmental Earth Sciences*, 80(5), 180. <https://doi.org/10.1007/s12665-021-09476-y>
- Wanyama, D., Moore, N. J., & Dahlin, K. M. (2020). Persistent vegetation greening and browning trends related to natural and human activities in the mount Elgon ecosystem. *Remote Sensing*, 12(13). <https://doi.org/10.3390/rs12132113>
- Yang, W., Seager, R., Cane, M. A., & Lyon, B. (2015). The annual cycle of East African precipitation. *Journal of Climate*, 28(6), 2385–2404. <https://doi.org/10.1175/JCLI-D-14-00484.1>
- Yirsaw, E., Wu, W., Shi, X., Temesgen, H., & Bekele, B. (2017). Land Use/Land Cover change modeling and the prediction of subsequent changes in ecosystem service values in a coastal

area of China, the Su-Xi-Chang region. *Sustainability (Switzerland)*, 9(7), 1–17.

<https://doi.org/10.3390/su9071204>

Zhou, F., Xu, Y., Chen, Y., Xu, C. Y., Gao, Y., & Du, J. (2013). Hydrological response to urbanization at different spatio-temporal scales simulated by coupling of CLUE-S and the SWAT model in the Yangtze River Delta region. *Journal of Hydrology*, 485, 113–125.

<https://doi.org/10.1016/j.jhydrol.2012.12.040>